Journal of Advances and Scholarly Researches in Allied Education
Vol. 13, Issue No. 1, April-2017, ISSN 2230-7540

An Investigation on Fission Fragment Angular Distribution

Sonu Rani[1]* Dr. Anil Kumar[2]

[1] Research Scholar of OPJS University, Churu, Rajasthan

[2] Associate Professor, OPJS University, Churu, Rajasthan

Abstract – We likewise completed fission fragment angular distribution estimations for 16O+194Pt response at energies around the Coulomb boundary. Piece rakish dissemination can give critical data about the auxiliary and factual parts of splitting elements. The sections were identified utilizing regular finder telescopes. Trial precise dispersions were fitted utilizing the correct articulations and rakish anisotropies were removed. SSPM figurings accepting normal estimations of excitation vitality and precise force couldn't clarify the exploratory anisotropies in the vitality extend contemplated. CN delivered in the pre-actinide area have practically identical neutron division energies and parting boundary statures, which improves the likelihood of multi-chance splitting. In such circumstances, parting can occur after a couple of nucleon outflow too and figurings accepting normal estimations of excitation vitality and rakish force may yield equivocal outcomes.

Keywords: Fission, Fragment, Angular, Distribution, Coulomb Boundary.

----------X----------

INTRODUCTION

Angular conveyance of the parting pieces in overwhelming particle instigated splitting is an important test to comprehend the elements of substantial particle impacts. Parting section angular appropriations were for the most part clarified by the SSPM. In SSPM, part an¬gular conveyance is identified with the precise energy (J) appropriation and the width (K0) of the K (projection of J along the atomic symmetry pivot) dispersion of the fissioning cores. K0 thusly is identified with the atomic temperature and compelling snapshot of inactivity at the seat point. This makes the precise circulation estimations a ground-breaking apparatus to comprehend the state of the fissioning cores at seat point and furthermore the angular force engaged with the combination procedure. It additionally replies to the dispersion procedure of gooey atomic medium amid the parting rot. Splitting piece angular appropriation has been generally used to test [1, 2] the elements of combination parting process in actinide locale. Test estimations over years have demonstrated that part precise conveyance is touchy to entrance channel parameters and additionally the statis¬tical parts of middle of the road framework as it develops in time. In this section we portray the information investigation, factual model estimations and results acquired from the piece angular appropriation estimations for 16O+194Pt response.

1. Fission cross segment and angular circulations

The parting yields for each edge were taken and were standardized by the screen detector kept at 40o degree. The deliberate parting piece angular appropriations were changed from research center to focus of-mass casing utilizing Viola systematics for symmetric parting [3]. Vitality misfortune revisions of the shaft in the half target thickness were connected before the transformation to focus of-mass. In overwhelming particle initiated splitting, the fragments are specially discharged in forward and in reverse bearings regarding the bar and the precise anistropy An is characterized as (or w(9o°)) where W(180°) is the differential splitting cross area at 180o and W(90o) is the equivalent at 90o (opposite to the shaft bearing). The differential parting cross segment was ascertained utilizing the articulation

$$W(\theta_{cm}) = \frac{d\sigma_{fis}}{d\Omega} = \frac{1}{2}\frac{Y_{fis}}{Y_{mon}}\frac{d\sigma_R}{d\Omega}(\theta_{lab})\frac{\Omega_{mon}}{\Omega_{fis}}G \qquad (6.1)$$

where G is the Jacobian of research center casing to focal point of-mass casing change, Yfis and Ymon are the yields recorded by the parting finder and screen (Rutherford) identifier, individually. Qfis and Amon are the strong edge subtended by the splitting locator and screen indicator, separately. ^f(0iab) is the differential Rutherford cross segment. It was expected that occasions recorded in the screen

finders were because of unadulterated Rutherford disseminating. Add up to splitting cross area was gotten by coordinating the differential cross segment This was finished by fitting the differential cross segment information utilizing the conditions

$$\frac{d\sigma_{fis}}{d\Omega}(\theta) = a + b \times cos^2\theta + c \times cos^4\theta \quad (6.2)$$

and,

$$\sigma(E) = 4\pi\left(a + \frac{b}{3} + \frac{c}{5}\right) \quad (6.3)$$

Table 6.1 demonstrates the trial splitting cross segment alongside the factual mistakes at various shaft (c.m.) energies.

Part precise dispersions (standardized differential cross segment plotted against focal point of-mass edge) at various shaft energies for the present framework are appeared in Fig. 6.1.

Table 6.1: Fission cross section for ^{16}O + ^{194}Pt reaction at different beam energies.

E_{C}.TO. (MeV)	$crfi_{SS}$ (mb)	*Vfiss* (error) (mb)
72.8	17.03	1 . 8
74.6	47.11	2.7
76.5	75.7	4.4
79.3	161.4	1 1 . 2
81.1	255.96	21.5
83.0	316.3	26.5

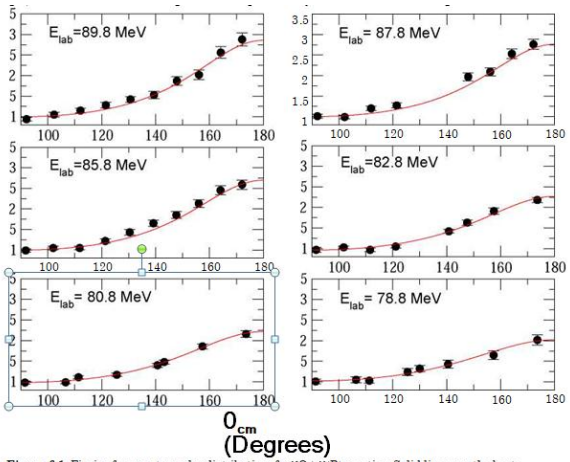

Figure 6.1: Fission fragment angular distributions for ^{16}O + ^{194}Pt reaction. Solid lines are the best fits to the angular distribution using the standard expressions [4, 5].

Table 6.2: Experimental fission fragment angular anisotropy in ^{16}O + ^{194}Pt reaction at different beam energies.

E_{c}.m.(MeV)	$A_{exp}t$	*A* (error)
72.8	1.9809	0.14
74.6	2.2556	0 . 1 2
76.5	2.3514	0.09
79.3	2.697	0 . 1 1
81.1	2.7628	0 . 1 2
83.0	2.8581	0.15

The precise circulations were fitted utilizing the standard articulations [4, 5]. In the standard hypothesis of parting section precise conveyances, it is expected that last course of pieces is given by the introduction of the atomic symmetry pivot as the core ignores the seat point. It is expected that core is framed at first in an arrangement inside the parting boundary. It is likewise expected that the Coriolis drive and different impacts disregarding the protection of K quantum number are of deficient solidarity to modify its incentive amid the quick plunge from seat to scission. Both these arguements are not legitimate for responses including heavier shots. Under the standard suppositions, angular dispersions can be spoken to by the symmetric best Parting section precise dissemination - Analysis and results wave capacities

$$W^{J}_{MK}(\theta) = \frac{2J+1}{4\pi}|D^{J}_{MK}(\phi,\theta,\psi)|^2 \quad (6.4)$$

where |DJMK(0,^,^)I are the symmetric best wave capacities. For turn zero cores, M, the turn projection, onto the bar pivot winds up zero and the above articulation decreases to

$$W^{J}_{0K}(\theta) = \frac{2J+1}{4\pi}|d^{J}_{0K}(\theta)|^2 \quad (6.5)$$

For contrasting and the trial information, it is important to average over J and K. Halpern and Strutinsky [6] inferred the articulation for K appropriation utilizing a steady temperature level thickness expecting the measurable arguements.

$$\rho(K) = \begin{cases} \frac{exp(\frac{-K^2}{2K_0^2})}{\sum_{K=-J}^{J} exp(\frac{-K^2}{2K_0^2})} & \text{for } K \leq J \\ 0 & \text{for } K > J \end{cases}$$

whereKq = , is the change of the K appropriation and Se//is the powerful snapshot of latency, talked about in area 2.4.1. Utilizing these, the angular dissemination of the sections can be spoken to as,

$$W(\theta) = \sum_{J=0}^{\infty}(2J+1)T_J \frac{\sum_{K=-J}^{J} \frac{1}{2}(2J+1)d^J_{0K}(\theta)^2 exp[\frac{-K^2}{2K_0^2(J)}]}{\sum_{K=-J}^{J} exp[\frac{-K^2}{2K_0^2(J)}]} \quad (6.6)$$

whereTj is the transmission coefficient for combination of the Jth incomplete wave and K0(J) is the standard deviation of the K appropriation for the J turn states. d-capacities were ascertained after strategy given in the ref. [5].

Parting section angular anisotropies (A = ^j^y) were acquired from the above fit. Table 6.2 gives the trial section anisotropy alongside mistakes at various pillar (c.m.) energies.

Statistical model examination

SSPM relates the section angular anisotropy to the precise force J at the seat point and the projection of this aggregate precise energy on the atomic symmetry hub K. In the rearranged shape the section angular anisotropy is given by the surmised articulation,

$$A = 1 + \frac{< l^2 >}{4K_0^2} \quad (6.7)$$

where K2 is the change of K appropriation, that is, the factual spread in K distri¬bution, clarified prior in this part. Bigger the estimation of K2, more isotropic will be the precise conveyance. In the event that the re-partition happens before the equilibration of K degrees of opportunity, the framework will have memory of its passage channel. In such cases, smaller will be the K dissemination, which prompts bigger anisotropy esteems. Such substantial anisotropy esteems were tentatively watched for some frameworks. The viable mo¬ment of inactivity, Ae//, relies upon the shape and consequently the disfigurement of the core at the seat point. Ae//is given by,

$$\frac{1}{\Im_{eff}} = \frac{1}{\Im_{\parallel}} - \frac{1}{\Im_{\perp}} \quad (6.8)$$

The seat point temperature T is computed utilizing Eq. 4.20. Erot were figured utilizing the Sierk remedy [7] dependent on the pivoting limited range demonstrate (RFRM). The mean square angular force estimations of the fissioning cores were figured utilizing factual model code PACE2 in follow back mode. As the CN 210Rn rot by means of splitting and molecule vanishing, one can't utilize the combination values straightforwardly in SSPM estimations. The combination/ - dispersions were gotten utilizing the coupled channel code CCFULL by fitting the test combination cross areas. This combination/ - appropriation was utilized as the contribution to PACE2 in follow back mode to get the splitting values. The CCFULL parameters utilized in the estimations for 16O + 194Pt response were talked about in section 4

In substantial particle incited combination responses the CN are shaped at high excitation vitality and angular energy. These hot, quickly turning cores rot to their ground state through molecule discharge, gamma outflow and parting. The opposition between different rot channels is represented by the transmission coefficients and level densities of the last states. The molecule discharge and splitting can happen from the CN itself or from its rot items until the point when the excitation vitality turns out to be not as much as molecule partition energies and parting obstruction, individually. At the point when the excitation vitality turns out to be not as much as partition vitality and splitting boundary vitality, gamma rot assumes control over the rot procedure. The rest of the excitation vitality and precise energy will be expelled along these lines. Parting can take palce from the CN itself or after the outflow of a couple of neutrons. In mass ~ 200 locale, the neutron division vitality and parting boundary are similar which help the multi-chance splitting to wind up a predominant rot channel. Amid the possibility splitting, when a neuton vanishes before the parting procedure it diminishes the CN excitation vitality by 8 - 10 MeV. In any case, the precise force diverted by the neutron dissipation is significantly less contrasted with the CN angular energy. The tentatively watched angular conveyance con¬tains commitment from different strides of this rot procedure and anisotropy counts accepting normal precise momenta and excitation energies may give uncertain outcomes.

Shell impacts additionally assume an exceptionally improtant job in splitting elements. It is notable that cores with enchantment proton or neutron numbers are more steadycomapared to non-enchantment cores. Single-molecule impacts are likewise in charge of numerous other commonplace atomic marvels. These incorporate the occurance of twisted instead of circular ground state shapes for mid-shell cores, the occurance of sec¬ondary least in the parting hindrances of numerous actinide cores and so on. These auxiliary minima are in charge of the occurance of parting isomers and middle of the road structures in splitting cross areas. The division of overwhelming cores at low excitation energies into sections of unequal mass is additionally accepted to be caused by these single molecule impacts. The sole explanation behind the presence of super-overwhelming cores (with vanishingly little fluid drop parting obstructions) are likewise because of the shell impacts in the potential vitality surface. In mass ~200 locale, shell adjustment may not prompt any noteworthy optional min¬ima in the atomic disfigurement potential vitality. This is because of the quick variety of LDM potential vitality with twisting. Nonetheless, huge shell adjustments to LDM potential at seat point were anticipated in this mass locale [8, 9]. The atomic dimension thickness parameter, a critical parameter in factual model

estimations, is additionally observed to be especially touchy to shell revisions. The dimension thickness parameter demonstrates a sensational decrease in its qualities close to the shell conclusion. Shell remedies at the seat point were not considered truly in numerous recently revealed works. This rectification is especially critical for the cores having huge ground state shell amendments around ACN = 210. Aradhana et al [10] announced atypical angular anisotropies in 12C + 198Pt framework and typical anisotropies in 12C + 194Pt . It was seen that the deliberate anisotropies were essentially bigger than SSPM calcula¬tions expecting normal excitation vitality and precise force and the deviations from the counts expanded with diminishing in vitality. The creators conjectured that shell impacts in potential vitality could be the conceivable purpose behind this irregular behav¬ior. Mahata et al [11] further expanded this examination, estimating parting section angular disseminations in 19F + 194>198Pt frameworks. 19F + 194Pt has a neutron shell conclusion (N = 126) which was relied upon to go astray from SSPM expectations if the prior speculations were right. Deviation from SSPM computations were seen at couple of energies for this framework. Factual model computations incoporating the multi-chance nature of parting and additionally shell rectifications at the seat point could clarify the trial anisotropies attractively. It was additionally seen that the re-examination of 12 C + 194,198Pt information, with multi-chance splitting considered in the figurings, lessened the difference between the test information from SSPM estimations extensively in 12C + 198Pt response.

In the present work, factual figurings were performed utilizing PACE2, with combination/ - dispersion as the info. The widening of angular force at close hindrance energies [12] were considered by including the rotational couplings of the objective cores. Fermi gas demonstrate was utilized to compute the dimension denisty parameters for ground state distortions and seat point disfigurements. As the dimension thickness parameter and splitting obstruction statures are delicate to the shell amendment, these parameters could be changed to fit the excitation capacities. Nonetheless, it was discovered that diverse arrangements of B/(/) and the proportion of level thickness parameter at seat point and balance distortion, give solid match to the test information. Consequently, notwithstanding the deliberate parting cross segment and ER cross segment, prefission multiplicities, vpre, were additionally used to compel the measurable parameters. To the best of our insight, vpre estimations of 16O + 194Pt framework are not detailed in writing. Consequently vpre values were gotten from the systematics of Saxena et al [13]. In the estimations, the vitality subordinate shell

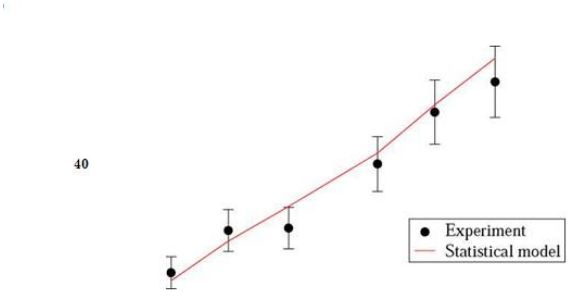

Figure 6.2: Fission probabilty for ^{16}O + ^{194}Pt reaction plotted against CN excitation energy. Solid line is the statistical model fit to the experimental data.

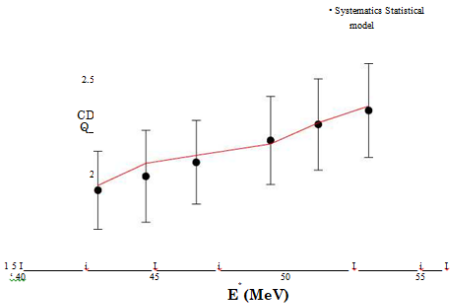

Figure 6.3: Pre-fission neutron multiplicities (obtained from the systematics) for ^{16}O + ^{194}Pt reaction plotted against CN excitation energy. Solid line is the statistical model fit.

Table 6.3: Different parameters used to obtain the fragment anisotropies at different beam energies. $E_{c.m.}$,< E >, Bf (l), E_{rot} and T are in MeV.

FJ	<*I*>	< *E* >	B/(0	E $_{RO}T$	*PFF*	K^2	ω >	*T*
72.8	11.4	2 2 . 6	8 . 0	0.565	82.31	49.39	156.2	0.60
74.6	14.0	23.0	7.83	0.913	82.35	50.23	226.6	0.61
76.5	16.3	24.5	7.69	1.191	82.41	55.21	298.96	0.67
79.3	19.6	26.5	7.34	1.857	82.59	61.21	425.5	0.74
81.1	21.7	27.4	7.14	2.245	82.74	63.71	516.1	0.77
83.0	23.4	28.2	7.04	2.452	82.83	67.92	560	0.82

adjustment shape (Ignatyuk level thickness parameter [14]) with asymptotic esteem — ^-was utilized for an. Shell remedies were consolidated in splitting hindrance and additionally in level thickness parameter in a deliberate way in the present examination. The type of the parting hindrance and level thickness parameters utilized in the figurings are given underneath.

$$B_f(l) = B_f^{RFRM}(l) - \Delta n + k\Delta n \tag{6.9}$$

$$a_n = \overline{a}[1 + \frac{\Delta n}{U}(1 - e^{-\eta U})] \tag{6.10}$$

$$a_f = (\frac{a_f}{a_n}) \times \overline{a}[1 + \frac{k\Delta n}{U}(1 - e^{-\eta U})] \tag{6.11}$$

where an, An and q are the fluid drop level thickness parameter, shell revision at ground state and damping factor, individually. k is the scaling element and kAn is the shell amendment at seat point distortion. k = 1 relate to square with shell redresses at the seat and balance misshapening.

Despite what might be expected k = 0 relate to zero shell remedy at seat point.

Utilizing the above solutions ER cross segment, parting likelihood and vpre esteems were at the same time fitted. The parting obstruction By(/) and ^ were changed amid this system. The best fit to the exploratory qualities were gotten for k = 0.762 and — = 0.983. Fig. 6.2 and Fig. 6.3 demonstrate the trial parting likelihood and neutron multiplicities plotted against CN excitation vitality. The strong line is the measurable model fit. Fig. 6.4 shows splitting cross areas contrasted and the factual model forecasts. SSPM counts were performed utilizing the normal excitation vitality and < I2 > values got from the PACE2 yield. Table 6.3 gives diverse parameters used to acquire the section anisotropies at various bar energies.

The SSPM computations expecting normal excitation vitality and precise energy esteems over predicted the angular anisotropies at higher energies. At lower excitation energies, in any case, the figuring's coordinated with trial results. It might be noticed that in the vitality go contemplated in the present trial, the commitment from the quick parting procedure was unimportant as the greatest angular force populated in the response was much lower than the basic precise energy at which the fluid drop splitting boundary vanishes. The pre-harmony splitting, another non-compound core process that happens when the temperature at the seat point winds up practically identical to the parting obstruction, likewise did not add to the piece angular appropriations in the present framework. The likelihood of occurance of pre-balance splitting is given by the surmised articulation,

Ppef = e-0'5T (6.12)

The most extreme likelihood of pre-harmony splitting in the vitality run examined in 16O + 194Pt response is under 2%. Fig. 6.5 demonstrates the trial anisotropies contrasted and SSPM counts accepting normal excitation vitality and angular energy.

As made reference to before in this part, when multi-chance splitting is an overwhelming rot process, estimations accepting normal estimations of E* and < I2 > give uncertain outcomes. The affectability of piece angular dispersions to splitting occuring after molecule emis¬sion from the CN has been called attention to long back in writing [4, 15, 16]. Consequently splitting part angular disseminations were figured utilizing the articulation

$$W(\theta) = \sum_{m,E^*} \sum_{J=0}^{J_{max}} \sigma_{fission}(m, E^*, J) \sum_{K=-J}^{J} \frac{(2J+1) \times |d^J_{0K}(\theta)|^2 \times exp[\frac{-K^2}{2K_0^2(J)}]}{\sum_{K=-J}^{J} exp[\frac{-K^2}{2K_0^2(J)}]} \quad (6.13)$$

The disseminations of the fissioning cores in various possibility (m) in (E*,J) space, Vfissicm(m, E*, J), were computed utilizing PACE2 as made reference to before. In any case, fis¬sion piece precise anisotropies computed utilizing the RFRM compelling snapshot of latency Aeff, overpredicted the information. As the measurable parameters were at that point settled

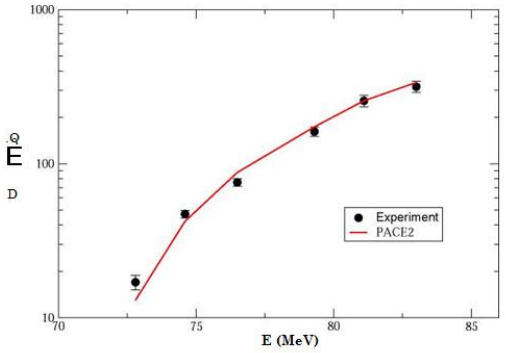

Figure 6.4: Experimental fission cross sections at different energies (centre-of-mass) compared with PACE predictions.

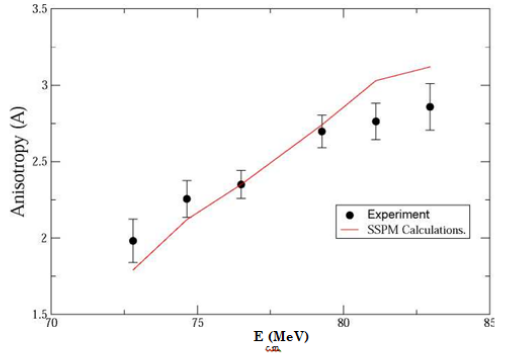

Figure 6.5: Fission fragment angular anisotropies in ^{16}O + ^{194}Pt reaction compared with SSPM calculations using average values of angular momentum and excitation energies.

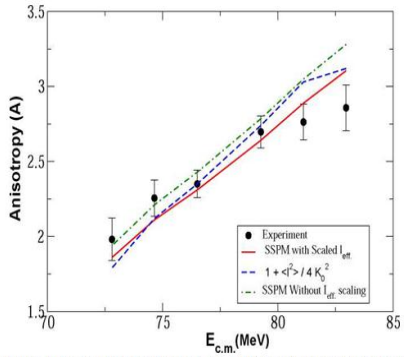

Figure 6.6: Fission fragment angular anisotropies in ^{16}O + ^{194}Pt reaction compared with SSPM calculations using average values of angular momentum and excitation energies, RFRM effective moment of inertia T_e// and T_e// increased by 10%.

in our computations, the anisotropies were fitted by scaling up the RFRM successful mo¬ment of latency. It was discovered that Ae//scaled up by a factor of 1.10 ±0.04 duplicated the exploratory anisotopies. The blunder in the scaling factor speaks to the standard deviation. Fig. 6.6 demonstrates the test anisotropies contrasted and hypothetical cal¬culations expecting normal estimations of < I2 > and E*, RFRM successful snapshot of inactivity Ae//and Ae//expanded by 10%.

CONCLUSION

The contradiction between trial results and SSPM figurings expecting average estimations of angular force and excitation energies affirmed the job of shell revisions at seat point in the computations. It was likewise understood that when the parting obstruction is tantamount with neutron partition energies, multi-chance nature must be considered in the estimations, as the tentatively watched angular distribution contains commitment from all means in the rot procedure. Definite factual examination uncovered that the ER cross areas and splitting probabilty can be fitted satisfactorily by various arrangements of £>/(/) and ^ values, which may not yield legitimate precise dispersions. It might be noticed that the vpre esteems were additionally affected by B/(l) and values. With the end goal to have unambiguous estimations of J appropriation and excitation energies, vpre values should likewise be fitted all the while to oblige the measurable model parameters. The test results likewise demonstrated that RFRM Qeff-esteem must be expanded by 10% to fit the anisotropy esteems. This outcome is steady with past estimations mass ~ 200 locale. It might be noticed that Of esteems were duplicated by 1.21 ±0.17 on account of 19F + 194Pt and 1.37 ±0.15 on account of 19F + 198Pt to fit the test results [11]. So also an increase factor of 1.54 ±0.12 and 0.96 ±0.10 were required to fit anisotropy esteems in 12C + 194Pt and 12C + 198Pt responses, individually. Normal scaling factor acquired for 19F + 188(192)Pt framework was 1.17 ±0.26 (1.39 ±0.18) [17]. The bigger Of qualities saw in these frameworks could suggest more reduced shapes at the seat point when contrasted with that anticipated by RFRM. However more test results are required to have a methodical comprehension of the job of multi-chance parting, shell conclusion and the shell adjustments at seat point, in combination splitting procedure.

REFERENCES

1. W. Reisdorf, F. P. Hessberger, K. D. Hildenbrand, S. Hofmann, G. Munzenberg, K. H. Schmidt, J. H. R. Schneider, W. F. W. Schneider, K. Summerer, G. Wirth, J. V. Kratz, and K. Schlitt (2002). Phys. Rev. Lett 49, p. 1811.

2. A. B. Balantekin, S. E. Koonin, and J. W. Negele (2003). Phys. Rev. C 28, p. 1565.

3. C. H. Dasso, S. Landowne, and A. Winther (2004). Nucl. Phys A 405, p. 381.

4. C. H. Dasso, S. Landowne, and A. Winther (2005). Nucl. Phys A 407, p. 221.

5. C. R. morton, A. C. Berriman, R. D. Butt, M. Dasgupta, D. J. Hinde, A. Godley, J. O. Newton, and K. Hagino (2011). Phys. Rev. C 64, p. 034604.

6. J. R. Leigh, M. Dasgupta, D. J. Hinde, J. C. Mein, C. R. Morton, R. C. Lemmon, J. P. Lestone, J. O. Newton, H. Timmers, J. X. Wei, and N. Rowley (1995). Phys. Rev. C 52, p. 3151.

7. A. M. Stefanini, M. Trotta, L. Corradi, A. M. Vinodkumar, F. Scarlassara, G. Mon- tagnoli, and S. Beghini, Phys. Rev. C 65, p. 034609 (2002).

8. C. L. Jiang, H. Esbensen, K. E. Rehm, B. B. Back, R. V. F. Janssens, J. A. Caggiano, P. Collon, J. Greene, A. M. Heinz, D. J. Henderson, I. Nishianaka, T. O. Pennington, and D. Seweryniak (2012). Phys. Rev. Lett 89, p. 052701.

9. A. M. Stefanini, L. Corradi, A. M. Vinodkumar, Y. Feng, F. Scarlassara, G. Mon- tagnoli, S. Beghini, and M. Bisogno (2000). Phys. Rev. C 62, p. 014601.

10. A. M. Stefanini, D. Ackermann, L. Corradi, D. R. Napoli, C. Petrache, P. Spolaore, P. Bednarczyk, H. Q. Zhang, S. Beghini, and G. Montagnoli (1995). Phys. Rev. Lett. 74, p. 864.

11. H. Timmers, D. Ackermann, S. Beghini, L. Corradi, J. H. He, G. Montagnoli, F. Scarlassara, A. M. Stefanini, and N. Rowley (1998). Nucl. Phys A 633, p. 421.

12. M. Dasgupta, D. J. Hinde, N. Rowley, and A. M. Stefanini (1998). Ann. Rev. Nucl. Part. Sci 48, p. 4017.

13. H. Timmers, J. R. Leigh, M. Dasgupta, D. J. Hinde, R. C. Lemmon, J. C. Mein, B. R. Morton, J. O. Newton, and N. Rowley (2002). Nucl. Phys A. 584, p. 190.

14. R. Stokstad (1985). In Treatise in Heavy-Ion Science, edited by D. A. Bromley, Vol. 3 (Plenum, New York, 1985).

15. P. Grange and H. A. Weidenmuller (2013). Phys. Lett. 96B, p. 26.

16. P. Grange, L. Jun-Quing, and H. A. Weidenmuller (1983). Phys. Rev C 27, p. 2063.

17. P. Grange, S. Hassani, H. A. Weidenmuller, A. Gavron, J. R. Nix, and A. J. Sierk (2012). Phys. Rev C 34, p. 209.

18. P. Grange (2014). Nucl. Phys A 428, p. 37c.

19. B. B. Back, D. J. Blumenthal, C. N. Davids, D. J. Henderson, R. Hermann, D. J. Hofman, C. L. Jiang, H. T. Penttila, and A. H. Wuosmaa (2014). Phys. Rev C 60, p. 044602.

20. P. D. Shidling, N. M. Badiger, S. Nath, R. Kumar, A. Jhingan, R. P. Singh, P. Sugathan, S. Muralithar, N. Madhavan, A. K. Sinha, S. Pal, S. Kailas, S. Verma, K. Kalita, S. Mandal, R. Singh, B. R. Behera, K. M. Varier, and M. C. Radhakrishna (2016). Phys. Rev. C 74, p. 064603.

21. P. D. Shidling, N. Madhavan, V. S. Ramamurthy, S. Nath, N. M. Badiger, S. Pal, A. K. Sinha, A. Jhingan, S. Muralithar, P. Sugathan, S. Kailas, B. R. Behera, R. Singh, K. M. Varier, and M. C. Radhakrishna (2008). Phys. Lett. B 670, p. 99.

22. K. T. Brinkmann, A. L. Caraley, B. J. Fineman, N. Gan, J. Velkovska, and R. L. McGrath (2014). Phys. Rev C50, p. 309.

23. L. Corradi, B. R. Behera, E. Fioretto, A. Gadia, A. Latina, A. M. Stefanini, S. Szil- ner, M. Trotta, T. Wu, S. Beghini, G. Montagnoli, F. Scarlassara, R. N. Sagaidak, S. N. Atutov, B. Mai, G. Stancari, L. Tomasetti, E. Mariotti, A. Khanbekyan, and S. Veronesi (2015). Phys. Rev. C 71, p. 014609.

24. D. J. Hinde, D. Hilscher, H. Rossner, B. Gebauer, M. Lehmann and M. Wilpert (2012). Phys. Rev. C 45, p. 1229.

25. J. O. Newton, D. J. Hinde, R. J. Charity, J. R. Leigh, J. J. M. Bokhorst, A. Chat- terjee, G. S. Foote, and S. Ogaza (2011). Nucl. Phys. A 483, p. 126.

26. L. C. Vaz, D. Logan, E. Duek, J. M. Alexander, M. F. Rivet, M. S. Zisman, M. Kaplan, and J. W. Ball (1984). Z. Phys. A 315, p. 169.

27. L. Schad, H. Ho, G. Y. Fan, B. Lindl, A. Pfoh, R. Wolski, and J. P. Wurm (1984). Z. Phys. A 316, p. 179.

28. I. Dioszegi, N. P. Shaw, I. Mazumdar, A. Hatzikoutelis, and P. Paul (2000). Phys. Rev. C 61, p. 024613.

29. D. J. Hofman, B. B. Back, I. Dioszegi, C. P. Montoya, S. Schadmand, R. Varma, and P. Paul (1994). Phys. Rev. Lett. 72, p. 470.

30. M. Thoennessen, D. R. Chakrabarthy, M. G.Herman, R. Butsch, and P. Paul (1987). Phys. Rev. Lett. 59, p. 2850.

Corresponding Author

Sonu Rani*

Research Scholar of OPJS University, Churu, Rajasthan